

EINGEGANGEN 02. Sep. 1998  
Date of Receipt: \_\_\_\_\_

GSI Exp. No. E040

### Proposal for an Experiment at GSI, Darmstadt

1. Title of Proposal: Nuclear astrophysics studies at the FRS-ESR: ground state and decay properties of neutron rich nuclei in the  $^{132}\text{Sn}$  region

New Proposal

Continuation of Previous Experiment  
(Exp. No.:.....)

2. Spokesperson:

Full Address:

Telephone/Fax:

email:

H. Schatz

GSI

2523

h.schatz@gsi.de

3. Participants:

Address:

Telephone:

email:

see proposal

4. GSI Contact Person:

H. Schatz

5. UNILAC:

SIS:

ESR:

6. Requested Beam Properties and Experimental Equipment:

a) Ion Species (Charge State if Needed):

$^{238}\text{U}$

b) Intensity (Particle nA):

$10^9$  ions/s

c) Energy (MeV/u):

750

d) Target Station:

FRS target

e) Special Requests on Beam Properties:

SIS cooler

f) Special Target Requirements:

—

g) Electronic Pool:

standard

h) GSI Computers:

"

i) Safety Requirements:

"

j) Further Assistance Requested from GSI:

no

7. Requested Beam Time (in Shifts of 8 Hours each)

Total: 21 FRS + 42 FRS u. ESR + 21 parasitic Number of Runs: 3

Preferred Dates: 1999 - 2000

Dates when you cannot run: /

8. Detailed description of the Proposal: Please attach an experiment description (max. 10 pages including figures) which should summarize the scientific justification and relevant technical details for the proposed experiment. For a continuation request, a brief status report of the previous as well as an outline of the future experiments should be given.

Date: \_\_\_\_\_

(Do not fill in)

GSI Exp.No.: \_\_\_\_\_

### SUPPLEMENTARY FORM FOR SAFETY ASPECTS OF A PROPOSAL

Title: Nuclear astrophysics studies at the FRS-ESR: ground state and decay properties...

Spokesperson: H. Schatz GSI-Contact Person: \_\_\_\_\_

#### 1. General Safety

- a. Do you use combustible or hazardous gases within your experiment (e.g. gas target, gas detectors)? Yes  No   
What sort of gases? Ar + Methan (10%)  
Which quantities or flow rates? 10e/h
- b. Do you use other dangerous (e.g. toxic, inflammable, biologically hazardous etc.) materials within your experiment? Yes  No   
What sort of materials? \_\_\_\_\_  
Which quantities? \_\_\_\_\_
- c. Is your vacuum set-up equipped with fragile parts like thin glass or foil windows etc. (danger of implosion)? Yes  No   
Brief description of the construction: standard Fenster an F4
- d. Is it intended to move heavy parts for setting-up your experiment or during the experiment? Yes  No   
Brief description of the equipment and working procedure: \_\_\_\_\_

#### 2. Radiation Safety

- a. Do you use radioactive sources or materials on-site? Yes  No   
What sources? \_\_\_\_\_  
Which activities? \_\_\_\_\_
- b. Is it intended to direct the beam through air or other gases? Yes  No   
Beam sort, energy, intensity: \_\_\_\_\_  
Distance through air or gas: \_\_\_\_\_

#### 3. Electrical/Laser Safety

- a. Do you use electrical instruments on-site? Yes  No   
Max. Voltage/max. current: 3 kV
- b. Do you use high-intensity radio frequency (RF) sources on-site? Yes  No   
Frequency region/power: \_\_\_\_\_
- c. Do you use lasers in your experiment? Yes  No   
Laser-type, max. power: \_\_\_\_\_

4. Is there any other special safety aspect to be considered in connection with your proposal? Yes  No

Date:

28.8.98

Spokesperson of the experiment:

H. Schatz

# Nuclear astrophysics studies at the FRS-ESR: ground state and decay properties of neutron-rich nuclei in the $^{132}\text{Sn}$ region

H. Schatz<sup>1</sup>, F. Attallah<sup>1</sup>, K. Beckert<sup>1</sup>, F. Bosch<sup>1</sup>, H. Eickhoff<sup>1</sup>, B. Franzke<sup>1</sup>, H. Geissel<sup>1</sup>, J. Gerl<sup>1</sup>, J. Görres<sup>6</sup>, M. Hannawald<sup>3</sup>, M. Hausmann<sup>1</sup>, F. Käppeler<sup>2</sup>, O. Klepper<sup>1</sup>, I. Klöckl<sup>3</sup>, K.-L. Kratz<sup>3</sup>, K. Langanke<sup>4</sup>, G. Münzenberg<sup>1</sup>, F. Nolden<sup>1</sup>, B. Pfeiffer<sup>3</sup>, T. Radon<sup>1</sup>, C. Scheidenberger<sup>1</sup>, K. Schmidt<sup>1</sup>, J. Stadlmann<sup>7</sup>, M. Steck<sup>1</sup>, K. Sümmerer<sup>1</sup>, F.-K. Thielemann<sup>5</sup>, H. Weick<sup>1</sup>, Th. Winkler<sup>1</sup>, M. Wiescher<sup>6</sup>

<sup>1</sup> GSI, Darmstadt, Germany

<sup>2</sup> Inst. für Kernphysik III, Forschungszentrum Karlsruhe, Germany

<sup>3</sup> Inst. für Kernchemie, Universität Mainz, Germany

<sup>4</sup> Universität Aarhus, Denmark

<sup>5</sup> Inst. für theoretische Physik, Universität Basel, Switzerland

<sup>6</sup> Dept. of Physics, University of Notre Dame, USA

<sup>7</sup> II. Physikalisches Institut, Universität Giessen, Germany

## I. ASTROPHYSICAL MOTIVATION

About half of the isotopes in the universe that are heavier than iron have been synthesized by rapid neutron captures (r-process). Yet, to date, the origin of these nuclei is still unknown and no astrophysical scenario has been identified with certainty as the r-process site. The most promising r-process scenario is the neutrino-heated high entropy bubble in core collapse supernovae, but models fail to provide naturally the high entropies required to produce the heaviest r-process nuclei. Other proposed sites like neutron star mergers or accretion-induced collapse of a white dwarf cannot be ruled out either [1,2].

A key element in the search for the r-process site are the properties of very neutron-rich nuclei far from stability down to neutron separation energies of 2 MeV - specifically masses,  $\beta$ -decay half-lives, neutron capture rates and probabilities for  $\beta$ -delayed neutron emission. Knowledge of these data provides the link between the observed solar abundance pattern of r-nuclei and the conditions at the r-process site and is therefore a prerequisite for the determination of r-process conditions independent from astrophysical models [3] as well as for testing any proposed r-process scenario. Reliable nuclear physics input allows furthermore to predict r-process abundances for unstable nuclei like  $^{232}\text{Th}$  that can serve as r-process chronometers. This is especially important in connection with recent observations of r-process elemental abundance distributions in very metal poor halo stars [4,5].

However, for most of the nuclei along or near the r-process path no experimental information is available, and nuclear physics input for r-process calculations is derived from theoretical models that are fitted to the properties of nuclei closer to stability. A so far unresolved issue is, whether these models can be applied for the very neutron-rich nuclei in the r-process path as new nuclear structure effects might occur far away from stability, for example due to shell quenching or the formation of neutron skins (see [6] and also [7] for recent theoretical results concerning the  $^{132}\text{Sn}$  region). This lack of reliable nuclear data for very neutron-rich nuclei is especially problematic for nuclei around  $^{132}\text{Sn}$ , which are involved in the synthesis of the isotopes in the  $A = 130$  peak of the solar r-process abundance distribution. On the one hand, r-process model predictions for solar isotopic abundances show severe deficiencies in this mass region [3,8], like the strong underproduction of nuclei with  $A = 113 - 124$  or the abundance spikes at  $A = 134$ ,  $A = 136$  and  $A = 138$  (see Fig. 1) that are not seen in the observed r-process abundance distribution.

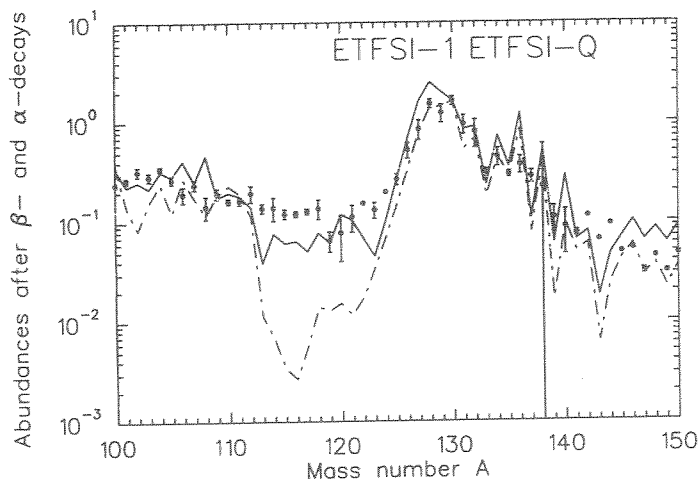


FIG. 1. The solar r-process abundances (dots) around  $A = 130$  compared to r-process calculations based on the ETFSI-1 (dot-dashed line) and the ETFSI-Q (solid line) mass models, respectively [5,9].

On the other hand it has been shown, that contrary to other mass regions, astrophysical freezeout effects do not have a strong impact in this region and that therefore the calculated abundance distribution directly reflects the

properties of the nuclei along the r-process path [1,2]. An improved knowledge of nuclear properties in this region would therefore strongly constrain astrophysical r-process scenarios.

We therefore propose to use the unique capabilities of the GSI accelerator facilities to produce very neutron-rich nuclei via projectile fission of  $^{238}\text{U}$  at relativistic energies and to investigate nuclei in the neighbourhood of  $^{132}\text{Sn}$ . In a first step, we plan to measure the probabilities for  $\beta$ -delayed neutron emission ( $P_n$ ) and the  $\beta$ -decay half-lives ( $T_{1/2}$ ) of 16 nuclei in the Cd - Xe region (see Fig. 2) with an accuracy of at least 10%. These measurements will be performed at the F4 focal plane of the FRS using the  $\beta$ -n coincidence technique.

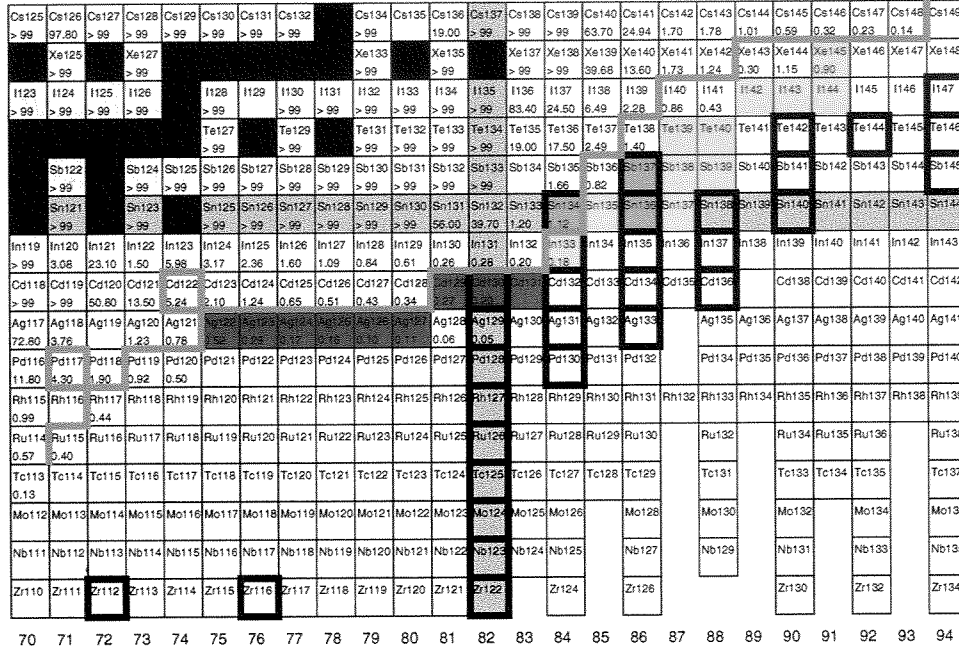


FIG. 2. The chart of nuclei showing neutron bound nuclei around  $^{132}\text{Sn}$ . The nuclei that we propose to investigate directly at the FRS are marked in orange (most important key isotopes) and yellow. For the red nuclei masses will be measured in the ESR in combination with the FRS.  $^{124}\text{Ag}$  and  $^{125}\text{Ag}$  will be investigated in both parts of the experiment. Stable isotopes are filled black and isotopes with a closed shell are filled grey. The r-process waiting points are framed with thick black lines. The border of measured masses [10] is indicated by the green line. Experimentally known half-lives are given in seconds and are written below the names of the isotopes.

For all of these nuclei the  $P_n$  values are experimentally unknown, except for  $^{134}\text{Sn}$ , where it is highly uncertain ( $17\% \pm 14\%$  [11]). In addition, for most of these nuclei the half-lives are unknown as well (see Fig. 2). Among the nuclei we propose to investigate are the astrophysically most important isotopes  $^{134}\text{Sn}$ ,  $^{136}\text{Sn}$  and  $^{137}\text{Sb}$ . These nuclei are waiting points in the r-process path and their properties are related to the problem of the  $A = 134, 136$  spikes in the predicted r-process abundances. These spikes are produced, since during the high neutron flux in the r-process relatively large abundances of the waiting point isotopes  $^{134}\text{Sn}$ ,  $^{136}\text{Sn}$ ,  $^{137}\text{Sb}$ , and  $^{138}\text{Sn}$  are accumulated. The half-lives of these nuclei are crucial since they determine how much material is accumulated - in steady flow the produced abundance is roughly proportional to the half-life. However, previous experiments revealed large discrepancies between experimental and theoretical half-lives. As an example, Fig. 3 shows that the QRPA predictions [12] for neutron-rich Sn isotopes seem to overpredict half-lives by a factor of 3–10.

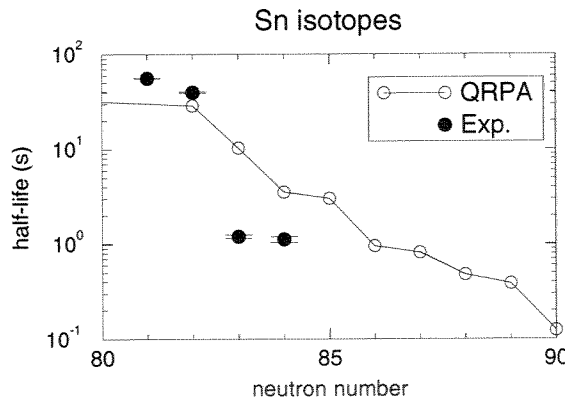


FIG. 3.  $\beta$ -decay half-lives for Sn isotopes. Shown are experimental data (Exp) as well as half-lives calculated with the QRPA and the FRDM 1992 mass model [12]

These calculations that are widely used in r-process calculations include allowed GT-decay only, and it has been pointed out that especially near  $^{132}\text{Sn}$  first forbidden transitions might enhance  $\beta$ -decay rates significantly [13]. More half-life measurements in this region will help to resolve this problem. After freeze out these waiting point nuclei decay mainly via  $^{134}\text{Sn}(\beta\dots)$ ,  $^{136}\text{Sn}(\beta n)^{135}\text{Sb}(\beta\dots)$ ,  $^{137}\text{Sb}(\beta n)^{136}\text{Te}(\beta\dots)$  and  $^{138}\text{Sn}(\beta n)^{137}\text{Sb}(\beta n)^{136}\text{Te}(\beta\dots)$  ( $\beta\dots$  denotes a sequence of  $\beta$ -decays until a stable nucleus is reached). Since the  $P_n$  value of  $^{134}\text{Sn}$  is only 14%, but the  $P_n$  values of  $^{137}\text{Sb}$  and  $^{138}\text{Sn}$  are predicted to be very large (99.91% and 100% respectively [12]), the decays of  $^{134}\text{Sn}$ ,  $^{137}\text{Sb}$  and  $^{138}\text{Sn}$  produce large amounts of nuclei with  $A = 134$  and  $136$ . On the other hand, the large predicted  $P_n$  value for  $^{136}\text{Sn}$  (99.99% [12]) prevents the decay of  $^{136}\text{Sn}$  from being an additional source for  $A = 136$  nuclei. However, the  $P_n$  values of  $^{134}\text{Sn}$ ,  $^{136}\text{Sn}$  and  $^{137}\text{Sb}$  are highly uncertain as can be seen in Fig. 4: all 3 nuclei are the first isotopes in their mass chain predicted to have a  $P_n$  value well above 90% but in all 3 mass chains the theoretical predictions strongly overestimate  $P_n$  values. Again, this might be due to the neglected first forbidden transitions. Indeed, in the case of  $^{136}\text{Sn}$  an estimate for  $P_n$  based on a combination of QRPA for allowed GT-decay and the gross theory for first forbidden transitions gives a much lower value of 25% [13].

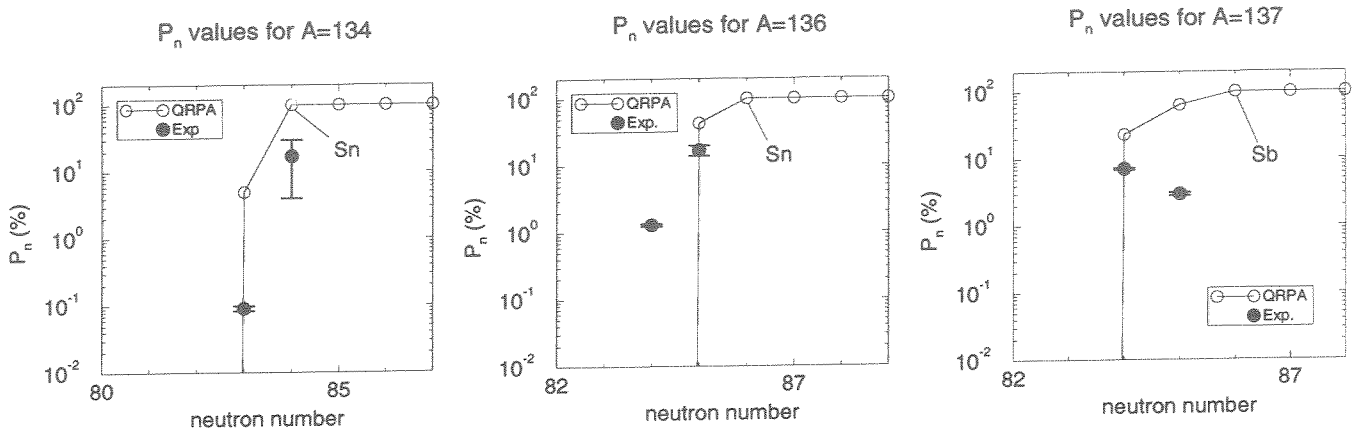


FIG. 4. Probabilities for  $\beta$ -delayed neutron emission  $P_n$ . Shown are experimental values (Exp.) and values calculated with the QRPA and the FRDM 1992 mass model [12]

The  $P_n$  value of  $^{139}\text{Sb}$  is of similar importance to the  $A = 138$  abundance spike and the measurement of  $P_n$  values of the other nuclei in this region will establish, whether the theoretical overprediction of  $P_n$  values and  $\beta$ -decay half-lives in this region is indeed a systematic trend. Therefore, experimental data obtained from the proposed experiment will for the first time allow to reliably calculate r-process abundances in the  $A = 134 - 138$  mass region.

After the determination of production cross sections, isotope separations and transmissions for nuclei in the neighbourhood of  $^{132}\text{Sn}$  at the FRS, we plan in a second step to inject some of these nuclei into the ESR for precise mass measurements. We propose to measure the masses of  $^{122-127}\text{Ag}$  and  $^{129-131}\text{Cd}$  (see Fig. 2) with an accuracy of at least 200 keV. The purpose of these mass measurements is twofold: Firstly, the r-process path is mainly determined by neutron separation energies, since during the r-process most nuclei within an isotopic chain are in  $(n, \gamma)$ - $(\gamma, n)$  equilibrium. Mass measurements of  $^{130}\text{Cd}$  and  $^{131}\text{Cd}$  will allow to determine the neutron separation energy of  $^{131}\text{Cd}$  and thereby the r-process path in this critical mass region. Secondly, this measurement will help to resolve one of the most striking problems in reproducing solar r-process abundances with astrophysical model calculations - the abundance trough at  $A = 113 - 124$  (see Fig. 1). This trough is a consequence of the behaviour of the nuclear masses in the region below the  $N = 82$  shell gap. It has been suggested that quenching of the  $N = 82$  shell far from stability might solve this problem [14]. This suggestion is motivated by the known quenching of the  $N = 20$  and  $N = 28$  shells (for example [15]) and by the prediction of this effect for the  $N = 82$  shell closure by HFB-Skyrme calculations [16]. Indeed, r-process calculations based on the ETFSI-Q mass model [17] that includes phenomenologically the shell quenching predicted by HFB-Skyrme calculations, clearly show an improved fit of the observed r-process abundance pattern (see Fig. 1 [5]). However, so far no conclusive experimental evidence exists for the quenching of the  $N = 82$  shell. First indications have been obtained from systematics of excitation energies of the first  $2^+$  and  $4^+$  states in Cd isotopes up to  $N = 80$  [9]. Another indication is the unexpectedly short measured half-life of  $^{130}\text{Cd}$  that can only be understood when a quenched  $N = 82$  shell is assumed [9]. The strongest hint for a  $N = 82$  shell quenching comes from the systematics of the masses of neutron-rich Cd isotopes. Fig. 5 shows the masses of Cd isotopes predicted by the FRDM 1992 mass model [18] (no shell quenching), the ETFSI-1 mass model [19] (no shell quenching) and the ETFSI-Q mass model (with shell quenching) in comparison with experimental data.

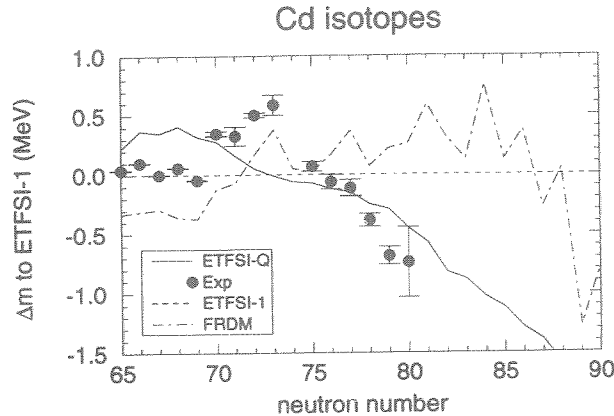


FIG. 5. The difference of the ETFSI-1 mass model predictions to the FRDM 1992 mass model, the ETFSI-Q mass model and the experimental data (Exp) [10] ( $M_{\text{ETFSI-1}} - M_i$ ) for neutron-rich Cd isotopes.

Clearly, a systematic deviation of the experimental masses from the mass model predictions without shell quenching in the direction of ETFSI-Q can be seen. However, these deviations are only marginally larger than typical mass model uncertainties ( $\approx 500$  keV). The proposed continuation of these mass measurements beyond the shell closure at  $^{130}\text{Cd}$  will determine, whether this trend persists and indeed points to a quenching of the  $N = 82$  shell. In the case of the Ag isotopes the experimental data are not yet within the range where shell quenching plays a role. Measuring the masses of  $^{122-127}\text{Ag}$  will reveal, whether a similar trend as for the Cd isotopes exists. It should be noted that for lighter nuclei the use of nuclear masses as a signature for shell quenching is a well established method (for example [15]).

## II. EXPERIMENTAL DETAILS

### A. Measurements of decay properties

$\beta$ -decay half-lives and probabilities for delayed neutron emission will be measured at the F4 focal plane of the FRS. An overview of the proposed setup is given in Fig. 6. The neutron-rich nuclei of interest are produced via projectile fission of a 750 MeV/u  $^{238}\text{U}$  beam impinging on a 1.25 g/cm<sup>2</sup> lead target. Various previous GSI experiments have demonstrated the feasibility of this method for the production of very neutron-rich nuclei (for example [20,21]) and the measured cross sections serve as an important basis for the planning of the proposed experiment. The secondary fission products are separated by mass and charge in the FRS via the  $B\rho - \Delta E - B\rho$  method. The standard detector set at the focal planes F2 and F4 serves to identify each transmitted fission product event-by-event by measuring magnetic rigidity, time of flight, energy deposition as well as position and direction of its trajectory. The fission products are then slowed down in a degrader and implanted into a stack of Si detectors at the F4 focal plane. The subsequent decays of the implanted nuclei are observed by detecting electrons in the Si detectors in coincidence with neutrons in a neutron long counter [22] surrounding the implantation area. The Si detectors will be segmented to allow for higher acceptable implantation rates and a clear correlation between an implanted nucleus and its decay (see for example [23] for details of this method). The neutron long counter consists of 3 concentric rings of  $^3\text{He}$  proportional gas counters embedded in a polyethylene moderator matrix and is capable to detect decay neutrons from fission products that have typical energies between 200 and 1000 keV with an efficiency of roughly 30%.

Probabilities for  $\beta$ -delayed neutron emission are determined from the ratio of implantations with a detected  $\beta$ -n coincidence to implantations without such a coincidence taking into account the known detector efficiencies.  $\beta$ -decay half-lives can be determined from the time structure of detected  $\beta$ 's and  $\beta$ -n coincidences. The neutron long counter has been successfully used in previous experiments at other facilities and its capability for  $P_n$  and  $T_{1/2}$  measurements of fission products has been demonstrated before [22,24]. The neutron background at the FRS had been measured previously with the same detector we plan to use. These measurements and the experience gained with the neutron long counter at other facilities show that neutron background will be sufficiently suppressed by using the  $\beta$ -n-nucleus coincidence technique thus allowing for measurements during the SIS spill.

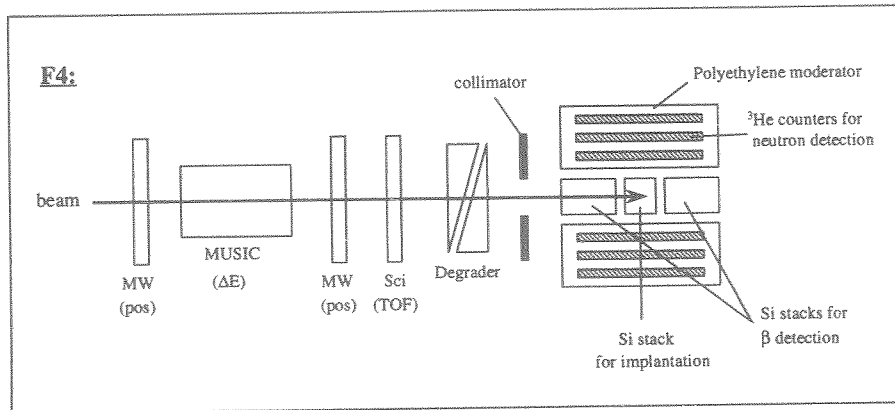


FIG. 6. Overview of the proposed experimental setup for the measurements of  $P_n$ -values and  $\beta$ -decay half-lives at the FRS focal plane F4.

### B. Measurements of ground state masses

Direct mass measurements of neutron-rich nuclei will be performed with the combination of FRS and ESR. The production mechanism is the same as described in the previous section. Neutron-rich nuclei will be separated in the FRS by the  $B\rho - \Delta E - B\rho$  method and then injected into the ESR. As can be seen in Tab. 1, all the isotopes of interest are relatively short lived with  $\beta$ -decay half-lives between 0.1 and 0.5 s. Therefore electron cooling cannot be applied and masses have to be determined using the isochronous mode of the ESR [25]. The revolution time of the nuclei circulating in the beam will then be measured either with the thin-foil time-of-flight detector [26] that was developed for this purpose or with a highly sensitive Schottky-pickup (e.g. resonant Schottky-pickup).

In a recent pilot experiment it has been demonstrated that the ESR can be operated in the isochronous mode with projectile fragments injected from the FRS [25]. In addition the mass resolution for uncooled Ni fragments has been measured using the Schottky technique. Based on these data we expect that together with a calibration of the ESR for particle velocities around the isochronous mode an accuracy of about 100 keV for mass measurements of nuclei with  $A \approx 130$  can be reached. New ion-optical calculations suggest that further improvements for the isochronous mode will be possible.

The time-of-flight detector has been installed in the ESR and recent test experiments demonstrated its ability to measure the revolution time of a single ion. These tests also showed that the number of turns for a circulating ion (on average 20, sometimes more than 100) is sufficiently large. However, the timing resolution and the detection efficiency will have to be improved.

The highly sensitive Schottky-pickup system will be developed in the near future. Depending on its performance and availability we will decide, which method (time-of-flight detector or Schottky-pickup) will be applied for which nucleus.

### III. INTENSITIES

For the measurement of the decay properties at the FRS, Tab. 1 lists the expected particle intensities as well as the rate of detected  $\beta$ -n coincidences for all nuclei of interest. These numbers are based on an incident  $^{238}\text{U}$  beam intensity of  $10^9$  ions/s and a lead target of  $1.25 \text{ g/cm}^2$  thickness. The production cross sections (see Tab. 1) have been taken from previous GSI experiments [20,27,28] except for  $^{127}\text{Ag}$ ,  $^{139}\text{Sb}$  and  $^{140}\text{Sb}$ , where the cross sections have been estimated assuming a decrease by a factor of 10 for each additional neutron. The particle transmissions have been calculated using the Monte Carlo code MOCADI and were 2% for the implantation into the Si-detector. The low transmission is a consequence of the large emittance due to the fission kinematics and includes also the nuclear reaction losses in the degrader and the detector material. The detection efficiency for  $\beta$ -n coincidences was assumed to be 20%.

Also shown in Tab. 1 are the expected intensities of nuclei to be injected into the ESR for mass measurements. Here the transmission from the target into the ESR was estimated to be 0.6%.

## IV. BEAM TIME REQUEST

### A. Measurements of decay properties

Based on the intensity estimates we request a total of 7 days of beam time for 1999 to perform the experiment at the FRS focal plane.

1999 : 2 days : optimization and calibration of FRS and detectors

5 days : measure all 16 nuclei shown in Fig. 2 with a statistics of  $\approx 1000$   $\beta$ -n coincidences.

With a primary beam intensity of  $10^9$  ions/s this will be sufficient to measure  $P_n$  values and  $\beta$ -decay half-lives of all of the 16 nuclei listed in Fig. 2 with a statistics of 1000  $\beta$ -n coincidences per isotope. This will allow to determine  $P_n$  values and  $\beta$ -decay half-lives with an accuracy of around 10%. The requested beam time will also include testing of the method by measuring  $^{90}\text{Br}$  and  $^{97}\text{Rb}$ , which have well known  $P_n$  values and large production yields (see Tab. 1).

### B. Measurements of ground state masses

For the second part of the proposed experiment, the mass measurements with a combination of FRS and ESR, we request 14 days of beam time for the year 2000:

2000: 4 days : optimization of FRS and ESR, calibration, particle identification

10 days : measure all 9 nuclei shown in Fig. 2 and Tab. 1

In addition to the requested beam time, 1 week of parasitic beam time will be necessary to prepare the experiment. During this time the injection into the ESR, the stability and reproducibility of the ESR in the isochronous mode and the performance of the frequency pickup system will be tested using nuclei with well known masses and half-lives.

TABLE I. Production cross sections ( $\sigma$ ),  $\beta$ -decay half-lives ( $T_{1/2}$ ), probabilities for delayed neutron emission ( $P_n$ ), ion rates (rate), and detected  $\beta$ -n coincidence event rates (n-events). The upper part of the table shows the data relevant for the implantation experiments. There, the ion rates refer to the implantation rate. The lower part of the table shows the data relevant for the mass measurements with the combination of FRS and ESR. Here the ion rates give the rate of injection into the ESR.  $\beta$ -decay half-lives and  $P_n$  values that are not experimental but calculated with the QRPA [12] are marked with <sup>a</sup>.

Isotope	$\sigma$ ( $\mu\text{b}$ )	$T_{1/2}$ (s)	$P_n$ (%)	rate ( $\text{s}^{-1}$ )	$\beta$ -n events ( $\text{s}^{-1}$ )
Decay measurements at the FRS					
$^{90}\text{Br}$	12771	1.92	25.2	928	47
$^{97}\text{Rb}$	2604	0.17	25.7	189	9.7
$^{134}\text{Sn}$	2400	1.12 <sup>a</sup>	17.0	174	5.9
$^{136}\text{Sn}$	12	0.95 <sup>a</sup>	100.0 <sup>a</sup>	0.87	0.17
$^{137}\text{Sb}$	160	1.05 <sup>a</sup>	99.9 <sup>a</sup>	12	2.3
$^{124}\text{Ag}$	138	0.17	1.2 <sup>a</sup>	10	0.025
$^{125}\text{Ag}$	37	0.16	5.29 <sup>a</sup>	2.7	0.028
$^{133}\text{In}$	3.3	0.18	100.0 <sup>a</sup>	0.24	0.048
$^{135}\text{Sn}$	189	3.0 <sup>a</sup>	98.5 <sup>a</sup>	14	2.7
$^{137}\text{Sn}$	1.2	0.81 <sup>a</sup>	99.3 <sup>a</sup>	0.087	0.017
$^{138}\text{Sb}$	16	0.041 <sup>a</sup>	19.7 <sup>a</sup>	1.2	0.046
$^{139}\text{Sb}$	3	1.05 <sup>a</sup>	99.8 <sup>a</sup>	0.22	0.043
$^{139}\text{Te}$	686	0.28 <sup>a</sup>	2.3 <sup>a</sup>	50	0.27
$^{140}\text{Te}$	72	0.29 <sup>a</sup>	2.9 <sup>a</sup>	5.2	0.030
$^{142}\text{I}$	229	0.20 <sup>a</sup>	47.8 <sup>a</sup>	16	1.6
$^{143}\text{I}$	15	0.14 <sup>a</sup>	77.2 <sup>a</sup>	1.1	0.17
$^{144}\text{I}$	3	0.062 <sup>a</sup>	35.6 <sup>a</sup>	0.22	0.016
$^{145}\text{Xe}$	59	0.9	3.0 <sup>a</sup>	4.3	0.025
Ground state mass measurements in the ESR					
$^{122}\text{Ag}$	1054	0.52		23	
$^{128}\text{Ag}$	370	0.29		8.1	
$^{124}\text{Ag}$	138	0.17		3.0	
$^{125}\text{Ag}$	37	0.16		0.8	
$^{126}\text{Ag}$	6	0.10		0.13	
$^{127}\text{Ag}$	0.6	0.11		0.013	
$^{129}\text{Cd}$	27	0.27		0.59	
$^{130}\text{Cd}$	6	0.20		0.13	
$^{131}\text{Cd}$	0.5	0.94 <sup>a</sup>		0.011	

- 
- [1] B. S. Meyer, *Ann. Rev. Astron. Astrophys.* **32**, 153 (1994).
- [2] C. Freiburghaus *et al.*, *Ap. J.*, accepted, (1998).
- [3] K. L. Kratz *et al.*, *Ap. J.* **403**, 216 (1993).
- [4] J. J. Cowan, M. Andrew, C. Sneden, and D. Burris, *Ap. J.* **480**, 246 (1997).
- [5] B. Pfeiffer, K.-L. Kratz, and F.-K. Thielemann, *Z. Phys. A* **357**, 235 (1997).
- [6] W. Nazarewicz, J. Dobaczewski, and T. R. Werner, *Phys. Scr.* **T56**, 9 (1995).
- [7] F. Hofman and H. Lenske, *Phys. Rev. C* **57**, 2281 (1998).
- [8] K. L. Kratz, B. Pfeiffer, and F. K. Thielemann, *Nucl. Phys. A* **630**, 352c (1998).
- [9] K.-L. Kratz, in *2nd International Conference on Exotic Nuclei and Atomic Masses, AIP Conference Proceedings* (American Institute of Physics, New York, 1998), to be published.
- [10] G. Audi and A. Wapstra, *Nucl. Phys. A* **595**, 409 (1995).
- [11] M. Asghar *et al.*, *Nucl. Phys. A* **247**, 359 (1975).
- [12] P. Möller, J. R. Nix, and K.-L. Kratz, *At. Data Nucl. Data Tab.* **66**, 131 (1997).
- [13] K. L. Kratz, B. Pfeiffer, and P. Möller, Technical report, Universität Mainz (unpublished).
- [14] B. Chen *et al.*, *Phys. Lett. B* **355**, 37 (1995).
- [15] N. A. Orr *et al.*, *Phys. Lett. B* **258**, 29 (1991).
- [16] J. Dobaczewski, W. Nazarewicz, and T. R. Werner, *Phys. Scr.* **T56**, 15 (1995).
- [17] J. M. Pearson, R. C. Nayak, and S. Goriely, *Phys. Lett. B* **387**, 455 (1996).
- [18] P. Möller, J. R. Nix, W. D. Myers, and W. J. Swiatecki, *At. Data Nucl. Data Tab.* **59**, 185 (1995).
- [19] Y. Aboussir, J. M. Pearson, A. K. Dutta, and F. Tondeur, *Nucl. Phys. A* **549**, 155 (1992).
- [20] M. Bernas *et al.*, *Phys. Lett. B* **331**, 19 (1994).
- [21] M. Bernas *et al.*, *Phys. Lett. B* **415**, 111 (1997).
- [22] O. Sorlin *et al.*, *Nucl. Phys. A* **583**, 763 (1995).
- [23] R. Schneider *et al.*, *Z. Phys. A* **348**, 241 (1994).
- [24] T. Mehren *et al.*, *Phys. Rev. Lett.* **77**, 458 (1996).
- [25] M. Hausmann *et al.*, GSI Scientific Report 1997, p. 170.  
M. Hausmann *et al.*, Proceedings of the Sixth European Particle Accelerator Conference (EPAC'98), <http://www.cern.ch/accelconf/e98/contents.html>  
H. Geissel *et al.*, Proceedings of the 2nd International Conference on Exotic Nuclei and Atomic Masses (ENAM98), GSI-Preprint-98-39, July 1998
- [26] J. Trötscher *et al.*, *Nucl. Instr. Meth. B* **70**, 455 (1992).
- [27] T. Enqvist, private communication, 1998.
- [28] C. Engelmann, Dissertation Universität Tübingen, GSI DISS.98-15, July 1998.